Biochemical Pharmacology 79 (2010) 1352–1362

Contents lists available at ScienceDirect

Biochemical Pharmacology

journal homepage: www.elsevier.com/locate/biochempharm

AMPK-mediated GSK3β inhibition by isoliquiritigenin contributes to protecting mitochondria against iron-catalyzed oxidative stress

Song Hwa Choi, Young Woo Kim, Sang Geon Kim *

Innovative Drug Research Center for Metabolic and Inflammatory Diseases, College of Pharmacy and Research Institute of Pharmaceutical Sciences, Seoul National University, Seoul 151-742, Republic of Korea

ARTICLE INFO

Article history:
Received 9 October 2009
Accepted 10 December 2009

Keywords:
Isoliquiritigenin
Mitochondrial dysfunction
Cytoprotection
GSK3β
AMPK

ABSTRACT

Isoliquiritigenin (ILQ), a flavonoid compound originated from *Glycyrrhiza* species, is known to activate SIRT1. Arachidonic acid (AA) in combination with iron (a catalyst of auto-oxidation) leads cells to produce excess reactive species with a change in mitochondrial permeability transition. In view of the importance of oxidative stress in cell death and inflammation, this study investigated the potential of ILQ to protect cells against the mitochondrial impairment induced by AA + iron and the underlying basis for this cytoprotection. Treatment with ILQ inhibited apoptosis induced by AA + iron, as evidenced by alterations in the levels of the proteins associated with cell viability: ILQ prevented a decrease in Bcl-x_L, and cleavage of poly(ADP-ribose)polymerase and procaspase-3. Moreover, ILQ inhibited the ability of AA + iron to elicit mitochondrial dysfunction. In addition, superoxide generation in mitochondria was attenuated by ILQ treatment. Consistently, ILQ prevented cellular H_2O_2 production increased by AA + iron, thereby enabling cells to restore GSH content. ILQ treatment enhanced inhibitory phosphorylation of glycogen synthase kinase-3β (GSK3β), and prevented a decrease in the GSK3β phosphorylation elicited by AA + iron, which contributed to protecting cells and mitochondria. GSK3β phosphorylation by ILQ was preceded by AMP-activated protein kinase (AMPK) activation, which was also responsible for mitochondrial protection, as shown by reversal of its effect in the experiments using a dominant negative mutant of AMPK and compound C. Moreover, the AMPK activation led to GSK3β phosphorylation. These results demonstrate that ILQ has the ability to protect cells from AA + iron-induced H_2O_2 production and mitochondrial dysfunction, which is mediated with GSK3β phosphorylation downstream of AMPK.

1. Introduction

Oxidative damage of the cell is a major factor for several human diseases. Excess reactive oxygen species (ROS) can modify membrane phospholipids, and result in cell and tissue injury [1]. Increased ROS and/or cytokines produced from inflammation promote oxidative modification of fatty acids within membrane phospholipids. The oxidation of fatty acids and phospholipids causes detrimental effects on cell signaling and activates phospholipase, which stimulates the release of arachidonic acid (AA), an ω-6 polyunsaturated fatty acid, and biologically active pro-inflammatory mediator [2]. In addition, AA can induce apoptosis by increasing the production of proapoptotic ceramide [3], calcium uptake into mitochondria [4], and excess ROS production via direct effects on mitochondria [5,6]. Moreover, AA in the presence of iron, a catalyst of auto-oxidation, increases oxidative damage of cells and the subsequent mitochondrial impairment [7]. Therefore, the combinatorial treatment of AA with iron exerts cell death in a synergistic manner, and this treatment may be utilized to study candidates that act against severe oxidative stress.

A several lines of evidence indicate that isoliquiritigenin (ILQ), a flavonoid with chalcone structure compound originated from *Glycyrrhiza* species (chemical structure shown in Fig. 1A), has

Abbreviations: AA, arachidonic acid; ACC, acetyl-CoA carboxylase; AICAR, 5-aminoimidazole-4-carboxamide-1-β-D-ribofuranoside; AMPK, AMP-activated protein kinase; CaMKK, calcium/calmodulin-dependent kinase kinase; DCFH-DA, 2′,7′-dichlorofluorescein diacetate; DPPH, 2,2-diphenyl-1-picrylhydrazyl; FACS, fluorescence-activated cell sorter; GSK3β, glycogen synthase kinase-3β; ILQ, isoliquiritigenin; Keap1, Kelch-like ECH-associated protein 1; LQ, liquiritigenin; MMP, mitochondrial membrane potential; mPTP, mitochondrial permeability transition pore; MTT, 3-(4,5-dimethylthiazol-2-yl)-2,5-diphenyl-tetrazolium bromide; Nrf2, NF-E2-related factor-2; NTA, nitrilotriacetic acid; Rh123, rhodamine 123; ROS, reactive oxygen species; SOD, superoxide dismutase; trolox, (±)-6-hydroxy-2,5,7,8-tetramethylchromane-2-carboxylic acid; VDAC, voltage-activated anion channel.

* Corresponding author at: College of Pharmacy, Seoul National University, Daehak-dong, Gwanak-gu, Seoul 151-742, Republic of Korea. Tel.: +82 2 880 7840; fax: +82 2 872 1795.
E-mail address: sgk@snu.ac.kr (S.G. Kim).

0006-2952/$ – see front matter © 2009 Elsevier Inc. All rights reserved.
doi:10.1016/j.bcp.2009.12.011

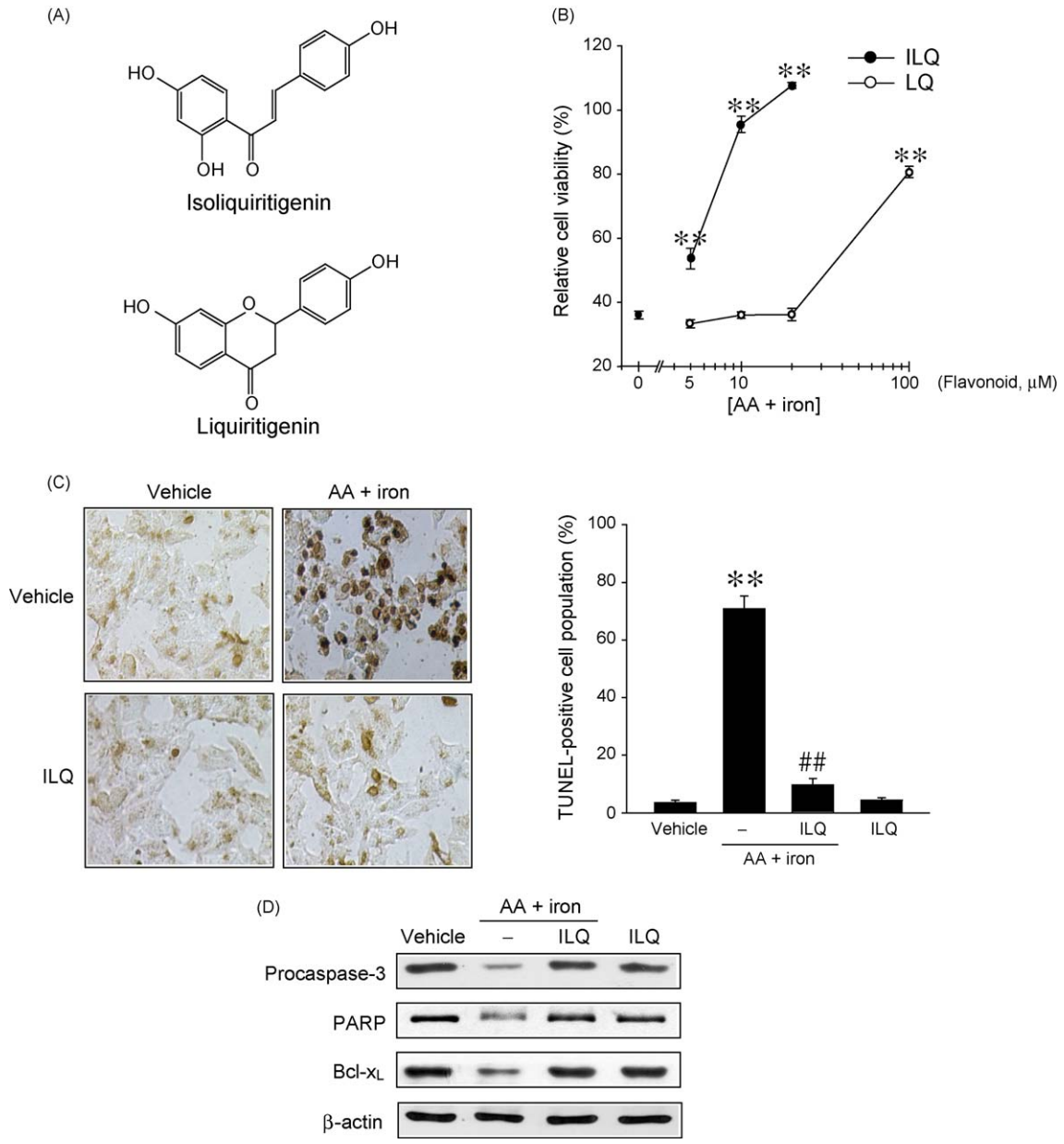

Fig. 1. Inhibition of AA + iron-induced apoptosis by ILQ. (A) The chemical structures of ILQ and LQ. (B) The effects of ILQ and LQ on cell viability. HepG2 cells were treated with several concentrations of ILQ or LQ for 1 h and were continuously incubated with 10 μM AA for 12 h, followed by exposure to 5 μM iron for 6 h. The dose-response effects of ILQ and LQ on cell viability were assessed using MTT assays. Data represent the mean ± S.E. of four separate experiments. For graphs in B and C, the statistical significance of differences between treatments and either the vehicle-treated control ($^{**}p < 0.01$) or cells treated with AA + iron ($^{\#\#}p < 0.01$) was determined. (C) TUNEL assay. HepG2 cells were treated with 20 μM ILQ for 1 h and were continuously incubated with 10 μM AA for 12 h, followed by exposure to 5 μM iron for 6 h. The percentage of TUNEL-positive cells (dark brown staining) was quantified. Data represent the mean ± S.E. of four separate experiments. (D) Immunoblottings for the proteins associated with apoptosis. Immunoblot analyses were performed on the lysates of HepG2 cells that had been incubated with 20 μM ILQ for 1 h, continuously treated with 10 μM AA for 12 h, and then exposed to 5 μM iron for 3 h. Equal protein loading was verified by β-actin immunoblotting. Results were confirmed by repeated experiments.

diverse pharmacological effects such as antioxidant [8–10], anti-inflammatory [11,12], anti-tumor [10,13,14], anti-platelet [15], and anti-peptic ulcer actions [16]. Also, ILQ is known as a SIRT1 activator, which is an upstream regulator of LKB1 [17,18]. In addition, treatment with ILQ alters conformation of Kelch-like ECH-associated protein 1 (Keap1) by alkylating specific cysteine residues, and thus results in NF-E2-related factor-2 (Nrf2) activation [19,20]. Nevertheless, other mechanistic basis for the antioxidant action of ILQ has not been elucidated.

Glycogen synthase kinase-3β (GSK3β) is a Ser/Thr kinase that is constitutively activated in normal state. In addition to the identification of GSK3β as a regulator of glycogen metabolism, other roles of this kinase as a regulator of cell function such as gene expression, cell cycle, and apoptosis have been recognized [21]. GSK3β is inactivated by phosphorylating the serine 9 residue [22], which may contribute to cell survival against ischemia/reperfusion injury by suppressing mitochondrial permeability transition pore (mPTP) opening [23,24]. This inhibitory phosphorylation of GSK3β at serine 9 also prevents phosphorylation of voltage-activated anion channel (VDAC), and promotes binding of GSK3β with adenine nucleotide translocase, resulting to interfere mPTP opening [25,26]. In our previous study, it has been shown that resveratrol treatment inhibited GSK3β activity downstream of AMP-activated protein kinase (AMPK) activation, which was responsible for mitochondrial protection [27].

AMPK, an intracellular sensor of energy status, may regulate cell survival or death in response to pathological conditions such as oxidative stress, hypoxia, and osmotic stress [7,28,29]. In mammalian cells, LKB1 and calcium/calmodulin-dependent kinase kinase (CaMKK) are the major upstream kinases of AMPK [30,31]. Treatment with AMPK activators [e.g., 5-aminoimidazole-4-carboxamide-1-β-D-ribofuranoside (AICAR) and metformin] increases cell viability under the conditions of stress [32,33]. Moreover, several cytoprotective agents not only induce antioxidant enzymes, but also decrease radical stress through AMPK activation [34]. For example, in our previous work, dithiolethiones were found to protect hepatocytes from oxidative stress induced by AA + iron through AMPK activation [7].

Currently, no information is available on whether ILQ has the ability to protect mitochondria and exerts a cytoprotective effect against oxidative burst. Moreover, the effects of ILQ on GSK3β and AMPK phosphorylations remain to be established. This study investigated whether ILQ has the ability to protect mitochondria from severe oxidative stress induced by AA + iron and thereby exert a cytoprotective effect and, if so, the mechanistic basis of its mitochondrial protective effect with particular reference to GSK3β and AMPK. Our work demonstrates that ILQ protects cells against iron-catalyzed severe oxidative stress by inhibiting mitochondrial impairment and ROS production, and that this cytoprotective effect results from GSK3β inhibition downstream of AMPK activation. In addition, the effect of liquiritigenin (LQ), another *Glycyrrhiza* component, on the mitochondrial function and cell death was comparatively examined.

2. Materials and methods

2.1. Materials

MitoSOX was supplied by Invitrogen (Carlsbad, CA). Anti-procaspase-3, anti-phospho-acetyl-CoA carboxylase (ACC), anti-phospho-AMPK, anti-GSK3β, anti-phospho-GSK3β, and anti-VDAC antibodies were obtained from Cell Signaling Technology (Beverly, MA). Antibodies directed against poly(ADP-ribose)polymerase (PARP), Bcl-x_L, and AMPK were purchased from Santa Cruz Biotechnology (Santa Cruz, CA). Horseradish peroxidase-conjugated goat anti-rabbit and goat anti-mouse IgGs were purchased from Zymed Laboratories (San Francisco, CA). SB216763 and compound C were obtained from Calbiochem (Darmstadt, Germany). DeadEnd™ Colorimetric TUNEL System was supplied from Promega (Madison, WI). ILQ, AA, ferric nitrate, nitrilotriacetic acid (NTA), 3-(4,5-dimethylthiazol-2-yl)-2,5-diphenyl-tetrazolium bromide (MTT), 2,2-diphenyl-1-picrylhydrazyl (DPPH), (±)-6-hydroxy-2,5,7,8-tetramethylchromane-2-carboxylic acid (trolox), rhodamine123 (Rh123), 2′,7′-dichlorofluorescein diacetate (DCFH-DA), anti-β-actin antibody, and other reagents were purchased from Sigma (St. Louis, MO). LQ was supplied from ChromaDex (Irvine, CA). The solution of iron–NTA complex was prepared as described previously [7].

2.2. Cell culture and treatment

HepG2 cells, a human hepatocyte-derived cell line, were obtained from ATCC (Rockville, MD) and were maintained in Dulbecco's modified Eagle's medium (DMEM) containing 10% fetal bovine serum (FBS), 50 units/ml penicillin and 50 μg/ml streptomycin at 37 °C in humidified atmosphere with 5% CO_2. For all experiments, cells (1×10^6) were plated in 10-cm (diameter) plastic dishes for 2–3 days (i.e., 80% confluency) and serum-starved for 24 h. Cells were incubated with 10 μM AA for 12 h, followed by additional exposure to 5 μM iron for the time period indicated in Section 3 or figure legends. To assess the effects of ILQ, the cells were treated with 5–20 μM ILQ for 1 h prior to incubation with AA + iron.

2.3. MTT assay

To measure cytotoxicity, HepG2 cells were plated at a density of 1×10^5 cells per well in a 48-well plate. After treatment, viable cells were stained with 0.25 mg/ml MTT for 2 h. The media was then removed, and formazan crystals produced in the wells were dissolved with the addition of 200 μl dimethylsulfoxide. Absorbance at 540 nm was measured using an ELISA microplate reader (Tecan, Research Triangle Park, NC). Cell viability was defined relative to untreated control [i.e., viability (%control) = 100 × (absorbance of treated sample)/(absorbance of control)].

2.4. TUNEL assay

TUNEL assay was performed using the DeadEnd™ Colorimetric TUNEL System, according to the manufacturer's instruction. HepG2 cells were fixed with 10% buffered formalin in PBS at room temperature for 30 min and were permeabilized with 0.2% Triton X-100 for 5 min. After washing with PBS, each sample was incubated with biotinylated nucleotide and terminal deoxynucleotidyltransferase in 100 μl equilibration buffer at 37 °C for 1 h. The reaction was stopped by immersing the samples in 2× saline sodium citrate buffer for 15 min. Endogenous peroxidases were blocked by immersing the samples in 0.3% H_2O_2 for 5 min. The samples were treated with 100 μl of horseradish peroxidase-labeled streptavidin solution (1:500) and were incubated for 30 min. Finally, the samples were developed using the chromogen, H_2O_2 and diaminobenzidine for 10 min. The samples were washed and examined under light microscope (200×). The counting of TUNEL-positive cells was repeated three times, and the percentage from each counting was calculated.

2.5. Immunoblot analysis

Cell lysates were prepared according to previously published methods [7]. Briefly, the cells were centrifuged at 3000 × *g* for 3 min and were allowed to expand osmotically to the point of lysis after the addition of lysis buffer. Lysates were centrifuged at 10,000 × *g* for 10 min to obtain supernatants and were stored at −70 °C until use. Immunoblot analysis was performed according to previously published procedures [7]. Protein bands of interest were developed using an ECL chemiluminescence system (Amersham, Buckinghamshire, UK). Equal protein loading was verified by immunoblotting for β-actin.

2.6. Flow cytometric analysis of mitochondrial membrane potential

Mitochondrial membrane potential (MMP) was measured with Rh123, a membrane-permeable cationic fluorescent dye using fluorescence-activated cell sorter (FACS). HepG2 cells were treated according to the individual experiment, stained with 0.05 μg/ml Rh123 for 1 h, and harvested by trypsinization. After washing with PBS containing 1% FBS, the change in MMP of cells was monitored using a BD FACS Calibur flow cytometer (San Jose, CA). In each analysis, 10,000 events were recorded.

2.7. Measurement of superoxide in mitochondria

MitoSOX is a live-cell-permeable and mitochondrial localizing superoxide indicator. After treatment of HepG2 cells with AA + iron, the cells were stained with 5 μM MitoSOX for 10 min

at 37 °C. Fluorescence intensity in the cells was measured using FACS. In each analysis, 10,000 events were recorded.

2.8. Measurement of H_2O_2 production

DCFH-DA is a cell-permeable non-fluorescent probe that is cleaved by intracellular esterases and is turned into the fluorescent dichlorofluorescein upon reaction with H_2O_2. The level of H_2O_2 generation was determined by the concomitant increase in dichlorofluorescein (DCF) fluorescence. After treatment, cells were stained with 10 μM DCFH-DA for 1 h at 37 °C. Fluorescence intensity in the cells was measured using FACS. In each analysis, 10,000 events were recorded.

2.9. Determination of reduced GSH content

Reduced GSH in the cells was quantified using a commercial GSH determination kit (Oxis International, Portland, OR, USA). Briefly, the GSH-400 method was a two-step chemical reaction. The first step led to the formation of substitution products (thioethers) between 4-chloro-1-methyl-7-trifluromethyl-quinolinum methylsulfate and all mercaptans present in the sample. The second step included β-elimination reaction under alkaline conditions. This reaction was mediated by 30% NaOH which specifically transformed the substituted product (thioether) obtained with GSH into a chromophoric thione.

2.10. Measurement of radical-scavenging activity

Radical-scavenging activity was measured using the DPPH method [35,36]. DPPH in methanol solution (150 μM) was added in each well, and were allowed to react with 3–1000 μM ILQ or trolox at room temperature in dark place. After 30 min, the absorbance values were measured at 515 nm using an ELISA microplate reader (Tecan, Research Triangle Park, NC). DPPH reduction rate was obtained from the following formula:

$$\text{DPPH reduction rate}(\%) = \frac{100(A_0 - A_s)}{A_0}$$

where A_0 was the absorbance of blank control, whereas A_s was the value for sample solution.

2.11. Recombinant adenoviral DN-AMPK construct and plasmid transfection

A plasmid encoding a dominant negative mutant of AMPKα (D157A; DN-AMPK) was kindly provided by Dr. J. Ha (Kyunghee University, Korea). To generate a recombinant adenovirus expressing DN-AMPKα, the construct was subcloned into the *attL*-containing shuttle plasmid, pENTR-BHRNX (Newgex, Seoul, Korea). Recombinant adenoviral DN-AMPKα was constructed and generated by using the pAd/CMV/V5-DEST gateway plasmid. HepG2 cells were infected with adenovirus diluted in DMEM containing 10% FBS at a multiplicity of infection (MOI) of 50 and incubated for 12 h. After removal of the viral suspension, cells were further incubated with DMEM containing 10% FBS for 2 days and then were treated with the indicated reagent. Adenovirus that expresses LacZ (Ad-LacZ) was used as an infection control. Efficiency of infection was consistently >90% with this method. The construct encoding for a kinase-dead mutant of GSK3β (KD-GSK3β) and a constitutive active form of GSK3β (S9A, CA-GSK3β) was kindly provided by Dr. J.R. Woodgett (Samuel Lunenfeld Research Institute, Ontario, Canada). Cells were transfected with the plasmids by using FuGENE HD (Roche, Indianapolis, IN). The empty plasmid, pCDNA3.1 was used for the mock transfection.

2.12. Preparation of mitochondrial fractions

Cells were homogenized in 5 mM Tris–HCl (pH 7.5) buffer containing 210 mM mannitol, 70 mM sucrose, and 1 mM EDTA. The homogenates were centrifuged twice at 1300 × *g* to remove pellet. The resulting supernatant was centrifuged at 15,000 × *g* to obtain the pellet containing mitochondria. The mitochondrial fractions were lysed in 10 mM Tris–HCl (pH 7.5) buffer containing 10 mM NaCl and 1.5 mM $MgCl_2$, and were subjected to immunoblot analysis.

2.13. Data analysis

Scanning densitometry was performed with an Image Scan & Analysis System (Alpha-Innotech Corporation, San Leandro, CA). One way analysis of variance (ANOVA) procedures were used to assess significant differences among treatment groups. For each treatment showing a statistically significant effect, the Newman–Keuls test was used for comparisons of multiple group means. The criterion for statistical significance was set at $p < 0.05$ or $p < 0.01$.

3. Results

3.1. Inhibition of AA + iron-induced apoptosis by ILQ

First, we used MTT assay to determine whether ILQ and LQ inhibited apoptosis induced by AA + iron. In the previous study, AA treatment (10 μM) induced oxidative stress and apoptosis, and iron (5 μM) enhanced the AA-induced toxicity in HepG2 cells [7]. Therefore, 10 μM AA and 5 μM iron were used in each of the experiments in the present study. In MTT assay, ILQ treatment (5–20 μM) protected cells against death induced by AA + iron. The maximal cytoprotective effect was observed at 20 μM (Fig. 1B). In contrast, LQ at the same concentrations was ineffective in protecting cells against AA + iron. One hundred μM of LQ was partially active (Fig. 1B). In subsequent experiments, ILQ was used as a cytoprotective candidate. TUNEL assay confirmed the protective effect of ILQ against toxicity elicited by AA + iron (Fig. 1C). AA + iron treatment stimulated PARP cleavage (shown as a decrease in full length PARP) and decreased the levels of procaspase-3 and Bcl-x_L, verifying that exposure of cells to AA + iron induced apoptosis. As expected, ILQ treatment significantly inhibited alterations in the levels of proteins associated with apoptosis (Fig. 1D). These results indicate that ILQ has the ability to protect cells against the synergized toxicity of AA + iron.

3.2. Inhibition of mitochondrial dysfunction by ILQ

In previous studies, it has been shown that AA impairs mitochondrial respiratory activity by inhibiting complexes I and III [5]. Thus, AA treatment causes dysfunction of mitochondrial membrane potential, inducing apoptosis of HepG2 and MH1C1 cells [6,7]. To correlate AA-induced apoptosis with alteration in mitochondrial function, MMP was measured using FACS after staining of the cells with Rh123. Rh123, a membrane-permeable cationic fluorescent, is used as a probe of MMP [37]. Low staining intensity of Rh123 represents mitochondrial damage and dysfunction. AA + iron treatment increased the number of cells in M1 fraction (fraction with low Rh123 fluorescence intensity), which indicates mitochondrial damage and dysfunction (Fig. 2A). Our results showed that AA + iron induced mitochondrial dysfunction and apoptosis. Although ILQ treatment (20 μM) slightly increased the population of M1 fraction, it inhibited the MMP dysfunction in response to a challenge by AA + iron, providing evidence that the cytoprotective effect of ILQ results from mitochondrial protection.

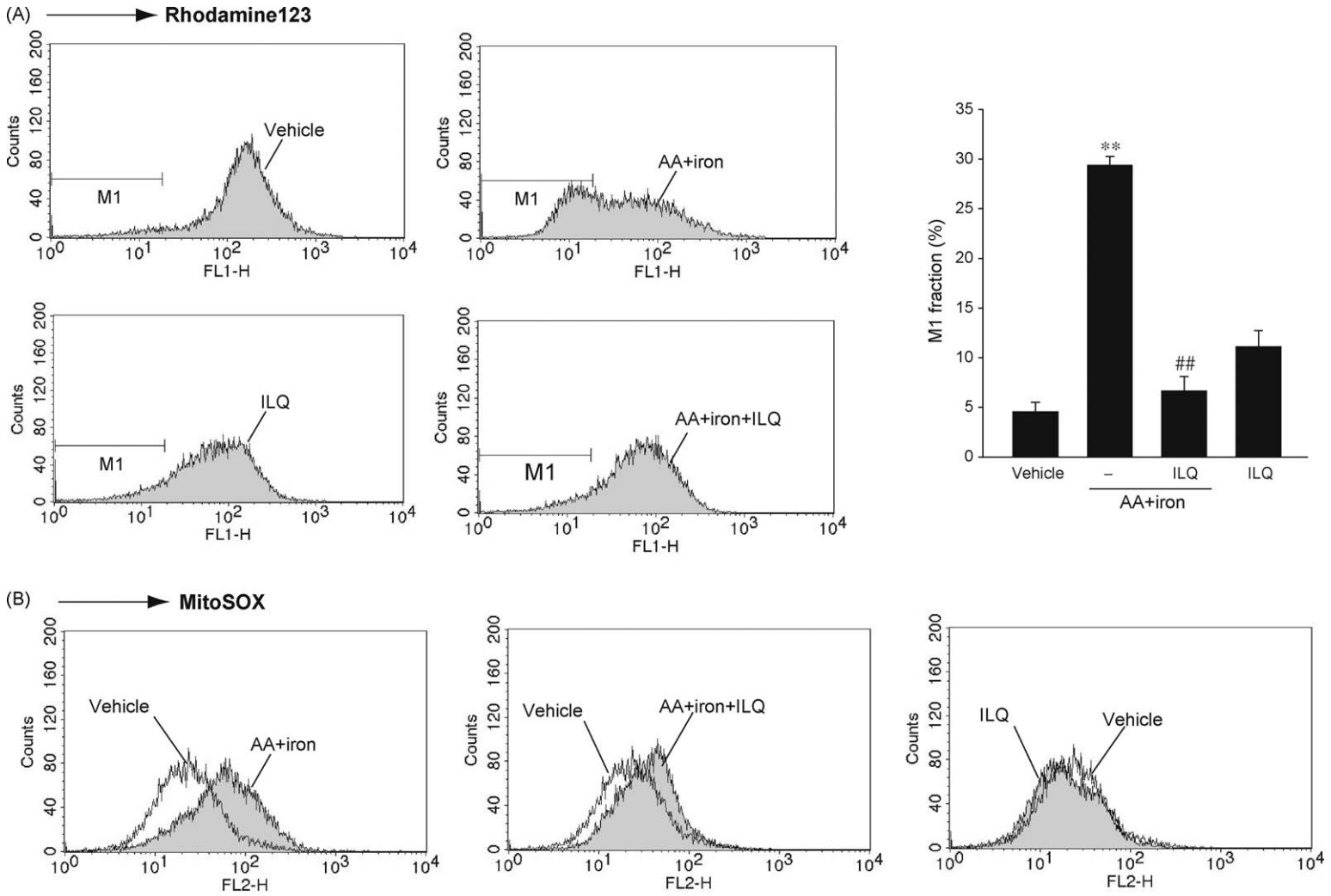

Fig. 2. Abrogation of mitochondrial dysfunction by ILQ. (A) Mitochondrial membrane permeability (MMP). HepG2 cells were treated with 20 μM ILQ for 1 h, followed by incubation with AA (12 h) and iron (1 h). The cells were harvested after Rh123 staining. Treatment of cells with AA + iron increased the subpopulation of M1 fraction (low Rh123 fluorescence), as indicated by the left shift of the population. Data represent the mean ± S.E. of three separate experiments. The statistical significance of differences between treatments and either the vehicle-treated control ($^{**}p < 0.01$) or cells treated with AA + iron ($^{\#\#}p < 0.01$) was determined. (B) Mitochondrial superoxide production. Cells were incubated with 20 μM ILQ for 1 h, treated with 10 μM AA (12 h) followed by incubation with 5 μM iron for 1 h, and then stained with MitoSOX. Increase in MitoSOX fluorescence indicates the production of mitochondrial superoxide. Treatment with ILQ attenuated the extent of mitochondrial ROS production elicited by AA + iron, as shown by decrease in MitoSOX fluorescence. Results were confirmed by repeated experiments.

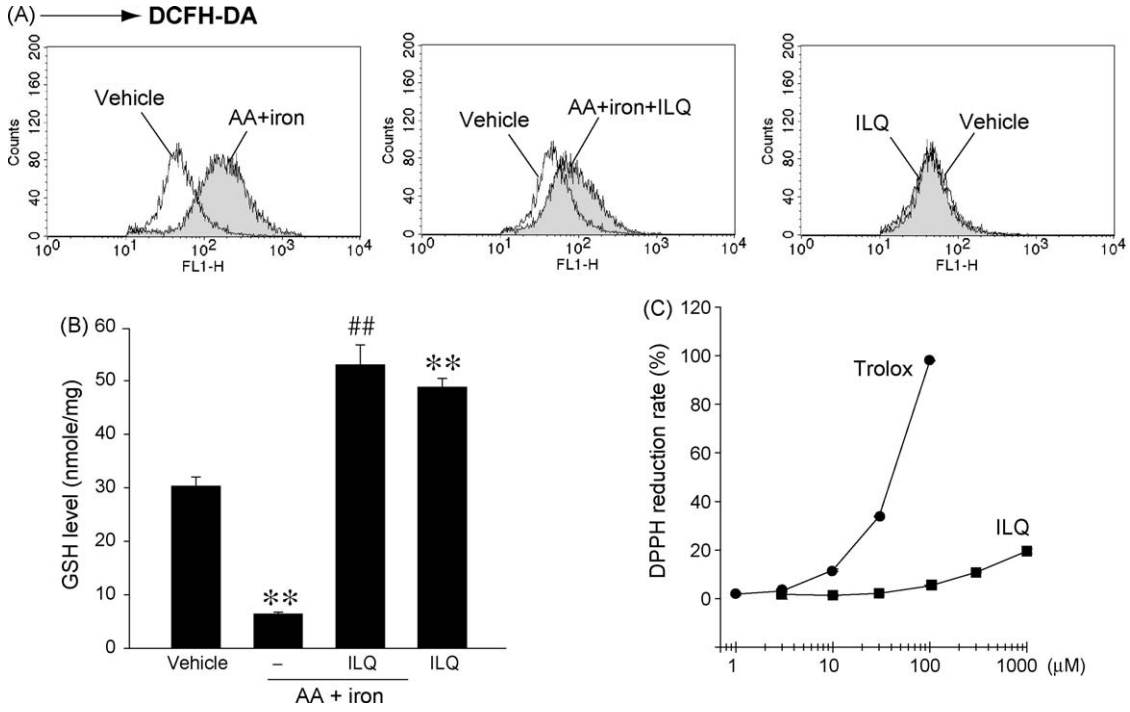

Fig. 3. The cellular antioxidant effect of ILQ. (A) Cellular H_2O_2 production. H_2O_2 production was monitored by measuring DCF fluorescence. HepG2 cells were incubated with 20 μM ILQ for 1 h, followed by incubation with AA (12 h) and iron (1 h). ILQ treatment attenuated AA + iron-induced ROS production. Results were confirmed by three separate experiments. (B) Cellular GSH content. The GSH content was assessed in cells that had been treated as described in the legend to Fig. 1D. Data represent the mean ± S.E. of three separate experiments. The statistical significance of differences between treatments and either the vehicle-treated control ($^{**}p < 0.01$) or cells treated with AA + iron ($^{\#\#}p < 0.01$) was determined. (C) *In vitro* radical-scavenging activity. Radical-scavenging activity was measured using the DPPH method, as described in Section 2. Results were confirmed by repeated experiments.

To further assess the effect of ILQ on mitochondria, we measured mitochondrial ROS production using MitoSOX, a live-cell-permeable and mitochondrial localizing superoxide indicator. Mitochondrial MitoSOX fluorescence was markedly increased by AA + iron treatment; however ILQ pretreatment inhibited mitochondrial superoxide production increased by AA + iron (Fig. 2B).

3.3. Cellular antioxidant effect of ILQ

The extent of intracellular H_2O_2 production was assessed by flow cytometric assay using DCFA-DA. Treatment of HepG2 cells with AA + iron increased H_2O_2 generation, which was completely antagonized by simultaneous ILQ treatment (Fig. 3A). Since GSH is an important endogenous antioxidant, deficiency of GSH increases ROS-induced toxicity [38]. Next, we assessed the level of GSH in the cells treated with AA + iron in combination with ILQ to determine the antioxidant effect of ILQ. Whereas the level of GSH is substantially decreased by AA + iron treatment, it was restored in cells concomitantly treated with ILQ (Fig. 3B). Moreover, ILQ treatment alone also promoted an increase in the GSH content compared to vehicle-treated control. To determine whether ILQ has a ROS scavenging capacity, DPPH assay was performed. Unlike trolox, a vitamin E analogue, ILQ failed to exhibit a radical-scavenging activity (Fig. 3C). The data support the hypothesis that the cytoprotective effect of ILQ may be associated with its antioxidative capacity, by which cells maintain redox-homeostasis via its regulation of cell signaling, rather than direct scavenging of ROS.

3.4. GSK3β phosphorylation and mitochondrial protection

It has been shown that GSK3β inhibition enables cells to protect mitochondria against ischemic/reperfusion injury and thereby contributes to cell viability [23,24]. In view of the critical role of GSK3β activity in mitochondrial protection, we examined the effect of ILQ on the inhibitory phosphorylation of GSK3β at serine 9 residue. Treatment of HepG2 cells with ILQ enhanced it in a time-dependent manner with significant increases being noted at later times (i.e., 6 or 12 h) (Fig. 4A). By contrast, exposure of cells to AA + iron (18 h) decreased the GSK3β phosphorylation, which was antagonized by simultaneous treatment with ILQ (Fig. 4B). The time-course effect of LQ treatment on the phosphorylation of GSK3β was also comparatively examined; LQ at 100 μM increased the GSK3β phosphorylation (Fig. 4C), whereas LQ at 20 μM failed to do so (data not shown). This result is consistent with its cytoprotective effect shown in Fig. 1B.

To assess the role of ILQ-induced GSK3β phosphorylation in protecting cells, GSK3β-inhibitory effect on cell viability was measured. A decrease in cell viability by AA + iron was significantly reversed by overexpression of KD-GSK3β (Fig. 5A). Consistently, the extent of cytotoxicity elicited by AA + iron was reduced by simultaneous treatment with SB216763 (a GSK3 inhibitor). To further correlate the GSK3β phosphorylation with mitochondrial function, MMP was measured using FACS after staining of the cells with Rh123. As expected, either KD-GSK3β transfection or SB216763 treatment inhibited the change in MMP induced by AA + iron (Fig. 5B). To test the role of GSK3β inhibition by ILQ in protecting mitochondria, the GSK3β-activating effect on cell populations of M1 fraction was measured using a construct encoding CA-GSK3β. The mitochondrial protective effect of ILQ was abrogated by CA-GSK3β transfection (Fig. 5C). A certain condition of oxidative stress such as ischemic/reperfusion injury has been shown to increase the mitochondrial content of GSK3β [26]. The level of GSK3β content in mitochondria was monitored in our cell model. As expected, treatment of cells with AA + iron notably increased GSK3β level in mitochondria, which was completely prevented by ILQ treatment (Fig. 5D). All of these results demonstrate that the cellular and mitochondrial protective

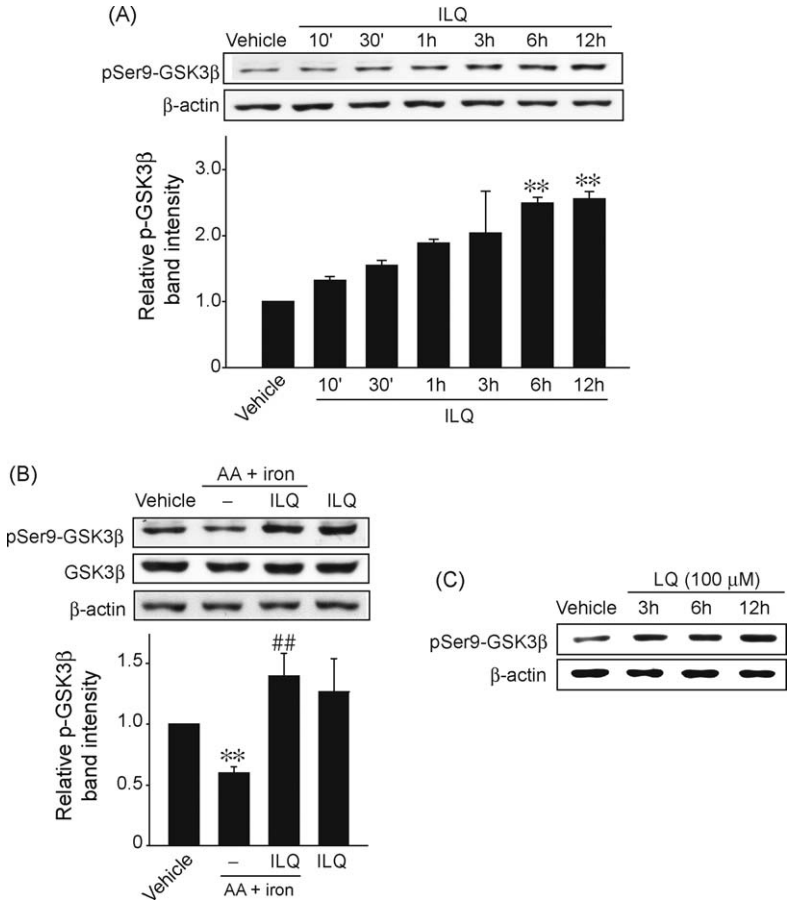

Fig. 4. Increase in GSK3β phosphorylation. (A) The time-course effect of ILQ on GSK3β phosphorylation. Immunoblotting for serine 9-phosphorylated GSK3β was performed on lysates of cells that had been treated with ILQ for the indicated time period. (B) Immunoblotting for serine 9-phosphorylated GSK3β. HepG2 cells were incubated with ILQ, as described in the legend to Fig. 1D. Immunoblotting for β-actin verified equal loading of proteins. Results were confirmed by three experiments. The statistical significance of differences between treatments and either the vehicle-treated control ($^{**}p < 0.01$) or cells treated with AA + iron ($^{\#\#}p < 0.01$) was determined. (C) The effect of LQ on the GSK3β phosphorylation.

effects of ILQ are associated with increase in the inhibitory phosphorylation of GSK3β.

3.5. AMPK activation by ILQ and its regulation of GSK3β phosphorylation

In our previous study, we found that AMPK plays a key role in protecting cells against iron-catalyzed oxidative stress [7,27,39]. In an effort to identify the upstream signal of GSK3β phosphorylation by ILQ, the time-course effects of ILQ on AMPK and ACC phosphorylations were assessed. In HepG2 cells, ILQ treatment resulted in notable increases in the phosphorylation of ACC at early times (10–30 min), which apparently preceded the GSK3β phosphorylation (Fig. 6A). Similarly, the phosphorylation of AMPKα was also increased by ILQ treatment, verifying AMPK activation. As expected, LQ treatment at 100 μM also increased the phosphorylations of AMPK and ACC (Fig. 6B). Twenty μM of LQ, however, failed to do so (data not shown).

To test the role of AMPK activation by ILQ in protecting mitochondria, the AMPK-inhibitory effect on cell populations of M1 fraction was measured. The mitochondrial protective effect of ILQ was abrogated by DN-AMPKα transfection or compound C (an AMPK inhibitor) treatment (Fig. 6C and D). Moreover, AMPK inhibition by either DN-AMPKα or compound C prevented the ability of ILQ to increase GSK3β phosphorylation (Fig. 7A), suggesting that AMPK regulates GSK3β activity. These results show that ILQ has a cytoprotective effect against severe oxidative stress induced by AA + iron and the ability to protect mitochondria, mediated through AMPK-dependent inhibitory phosphorylation of GSK3β (Fig. 7B).

4. Discussion

Excess iron deposition in the body causes injury to and dysfunction of target organs. Because the liver is the primary organ for iron storage, it is more sensitively affected by iron-overload [40]. In the early stage of pathological process, accumulation of excess iron in the non-parenchymal cells causes oxidative stress in the liver. Simultaneously, iron is redistributed toward surrounding hepatocytes. In addition, pro-inflammatory cytokines produced by activated macrophages may amplify ROS production and hepatocyte injury under iron-overload conditions [41,42]. In our previous study, we established a combinational treatment of iron and AA as an iron-catalyzed oxidative stress model and the associated signaling pathway [39]. Here, we report that ILQ has a cytoprotective effect against iron-catalyzed oxidative burst, as confirmed by the inhibition of apoptosis and alterations in apoptotic markers, which implies that ILQ may be beneficial for iron-overload liver disease.

Since mitochondria function as a stress sensor, they determine fate of the cell between apoptosis and cell survival process [43]. Within the mitochondrion, ROS is mainly produced in the respiratory chain [1]. AA is a pro-inflammatory fatty acid generated from cell membranes. AA initiates ROS generation and thus stimulates lipid peroxidation [44]. AA-induced oxidative stress has a direct effect on mitochondria [5,6]. Hence, AA treatment causes

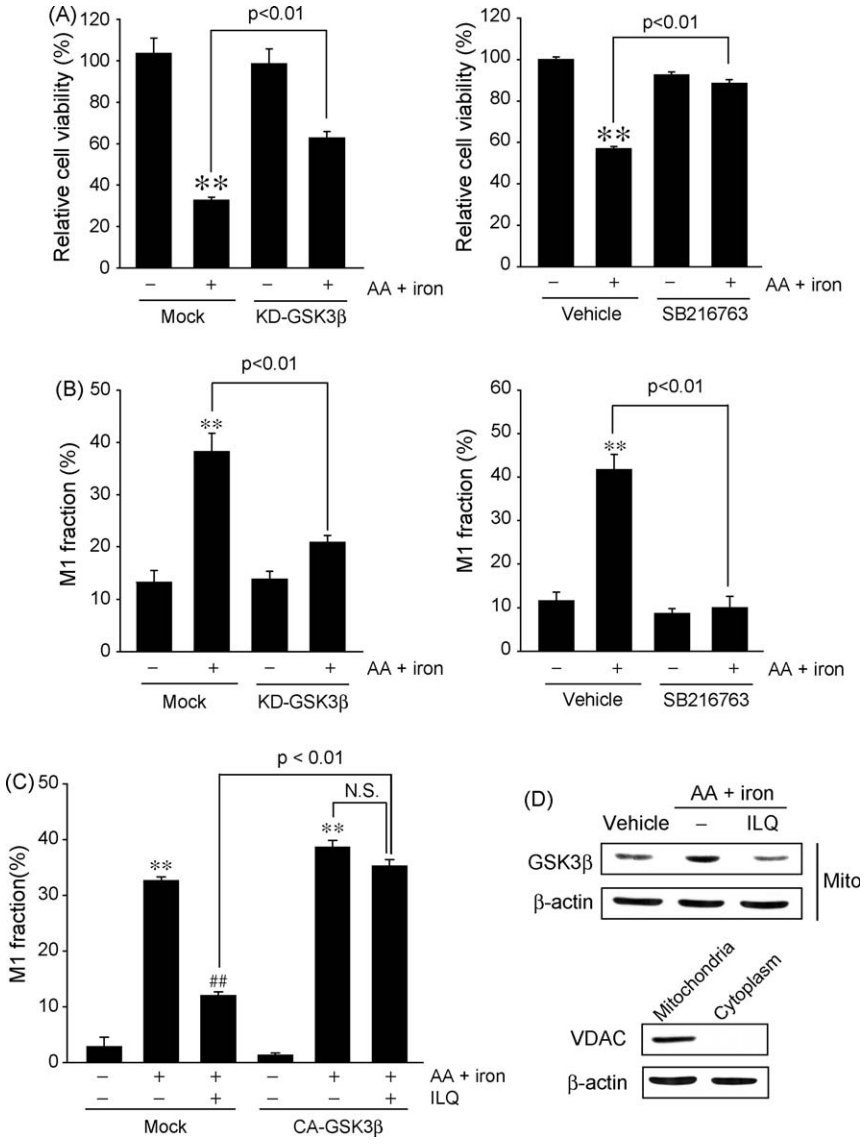

Fig. 5. The effect of GSK3β inhibition on cell viability and mitochondrial function. (A) The effect of GSK3β inhibition on the viability of cells. HepG2 cells that had been transfected with the plasmid encoding for KD-GSK3β or incubated with SB216763 (10 μM, for 1 h) were continuously incubated in a medium containing AA (12 h) and iron (1 h). Cell viability was analyzed by MTT assay. Data represent the mean ± S.E. of four separate experiments. (B) The effect of GSK3β inhibition on MMP transition. MMP was analyzed in cells that had been treated as described above. Data represent the mean ± S.E. of three separate experiments. (C) Reversal by CA-GSK3β of the ability of ILQ to restore MMP. MMP was analyzed in cells that had been treated as described above. Data represent the mean ± S.E. of three separate experiments. The statistical significance of differences between treatments and either the vehicle-treated control (**$p < 0.01$) or cells treated with AA + iron (##$p < 0.01$) was determined. N.S., not significant. (D) Immunoblottings for GSK3β in mitochondrial fractions. HepG2 cells were incubated with ILQ, as described in the legend to Fig. 1D. Immunoblotting for VDAC verified the purity of mitochondrial fractions. Results were confirmed by repeated experiments. Mito, mitochondria.

mitochondrial swelling and has an effect on mPTP opening [6]. In the present study, we found that ILQ as a natural flavonoid had the ability to inhibit ROS production and mitochondrial permeability transition, thereby protecting the key organelle. Our result showing the abrogation of superoxide production in mitochondria by ILQ suggests that the target of ILQ may reside in the organelle.

Co-treatment of cells with AA and iron enhances superoxide production in mitochondria, as shown by the MitoSOX assay [7]. Moreover, AA-induced ROS production in combination with iron catalysis amplifies oxidative stress and injury in cells. The prevention of AA + iron-induced MMP increase by cyclosporin A, an inhibitor of mPTP formation, suggests that mitochondrial dysfunction and the consequent generation of excess ROS may play a role in cell death [7]. In the present study, ILQ effectively antagonized DCFH oxidation, supporting its cellular H_2O_2-scavenging effect. In addition, ILQ was capable of preventing a decrease in cellular GSH content by AA + iron, further strengthening its antioxidative capacity. Our work provides evidence that the mitochondrial protection and the antioxidant effect of ILQ contribute to cell viability. Since PEG-SOD, PEG-catalase, Trolox or *N*-acetyl-L-cysteine antagonize the ability of AA + iron to induce ROS and apoptosis [7], this evidence provides additional support for the role of antioxidative action of ILQ in MMP transition and apoptosis.

Oxidative stress activates GSK3β and leads GSK3β to translocate into the mitochondria. Activated GSK3β in mitochondria then binds to and phosphorylates the components of mitochondrial membrane pore (e.g., VDAC and ANT), and thereby induces MMP transition [25,26]. Thus, GSK3β acts as the kinase crucial for the regulation of MMP transition [45]. Our results demonstrate that ILQ promoted inhibitory phosphorylation of GSK3β under the regulation of AMPK, which is in line with the previous observation that AICAR treatment increased GSK3β phosphorylation at serine 9 [46]. An important finding of this study is that the ability of ILQ to

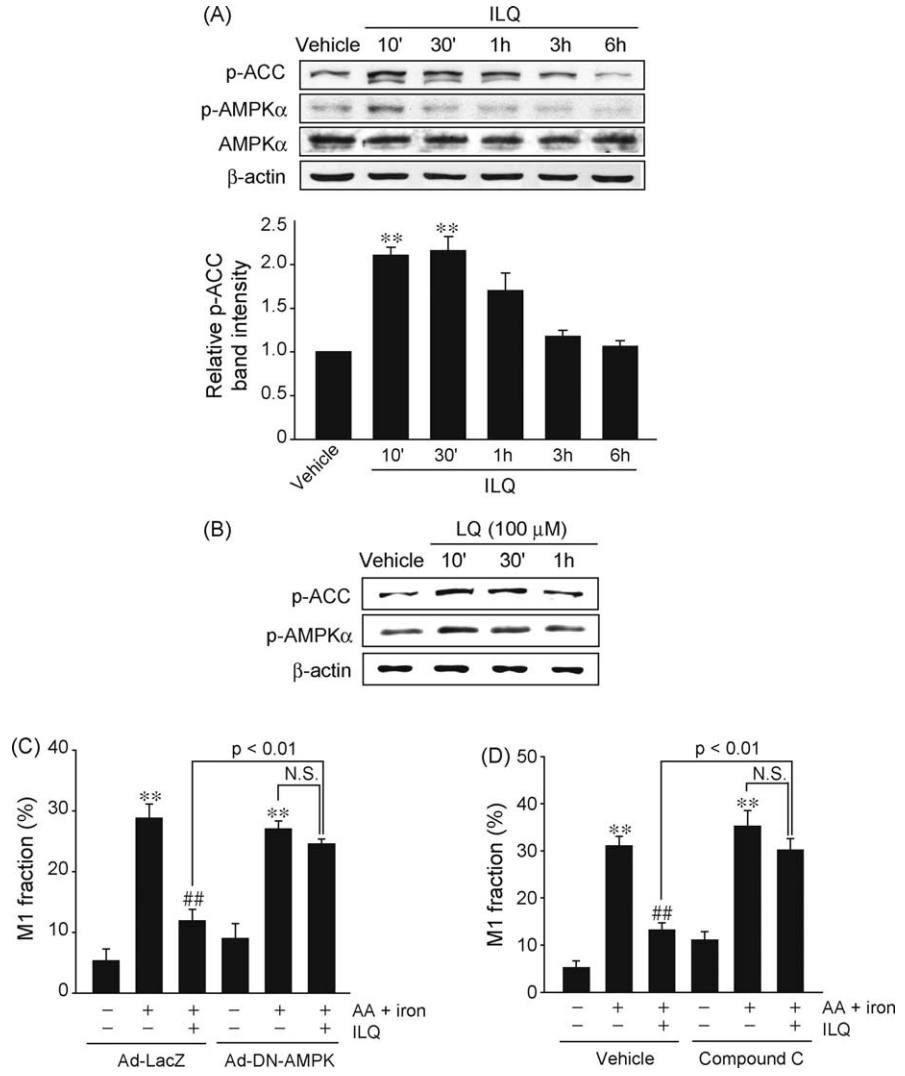

Fig. 6. AMPK activation by ILQ and its role in mitochondrial function. (A) AMPK activation by ILQ. Immunoblot analyses were performed on lysates of cells that had been treated with ILQ for the indicated time period. Results were confirmed by three separate experiments. (B) The effect of LQ on the phosphorylations of ACC and AMPK. (C) Reversal by Ad-DN-AMPKα of the ability of ILQ to restore MMP. After Ad-LacZ or Ad-DN-AMPKα infection (48 h), HepG2 cells were incubated with ILQ for 1 h and continuously exposed to AA (12 h) + iron (1 h). MMP was analyzed as described in the legend to Fig. 2A. Data represent the mean ± S.E. of three separate experiments. The statistical significance of differences between treatments and either the vehicle-treated control ($^{**}p < 0.01$), cells treated with AA + iron ($^{\#\#}p < 0.01$), or cells treated with AA + iron after Ad-DN-AMPK infection was determined. (D) Reversal by compound C of the effect of ILQ to restore MMP. After compound C treatment (3 μM, 30 min), cells were incubated with ILQ for 1 h, followed by incubation with AA (12 h) + iron (1 h). Data represent the mean ± S.E. of four separate experiments. The statistical significance of differences between treatments and either the vehicle-treated control ($^{**}p < 0.01$), cells treated with AA + iron ($^{\#\#}p < 0.01$), or cells treated with AA + iron after compound C treatment was determined. N.S., not significant.

protect mitochondria depends on the GSK3β phosphorylation. Resveratrol had a similar cytoprotective effect in association with the GSK3β phosphorylation [27]. Overall, these results corroborate the strong association of GSK3β inhibition by ILQ with mitochondrial protection.

AMPK is an energy sensing molecule that monitors cellular energy status by responding to changes in the AMP:ATP ratio [47]. AMPK activated by increased AMP/ATP ratio reserves cellular energy content, repressing ATP consumption with an increase in ATP synthesis. The activation of AMPK through phosphorylation regulates apoptosis in response to energy depletion by inhibiting anabolic pathways and stimulating catabolic processes [47]. The expression of PGC-1α and MnSOD mRNAs is elevated by treatment with an AMPK activator, which may inhibit ROS production in mitochondria [48]. Previous work in our laboratory showed that 1,2-dithiole-3-thiones protect cells from AA + iron-induced ROS production and mitochondrial dysfunction via AMPK activation [7]. In addition, there was crucial evidence for the role of AMPK activation in protecting mitochondria; the experiment using AICAR, an AMPK activator, elicited a similar cytoprotective effect [7]. Consistently, ILQ treatment also activated AMPK, which contributed to inhibitory phosphorylation of GSK3β, and consequently mitochondrial protection.

It has been shown that ILQ activated SIRT1 which was claimed to be the upstream regulator of LKB1 [17,18]. Also SIRT1 regulates lipid metabolism through LKB1-dependent AMPK activation [49]. Although the cytoprotective mechanism of ILQ involves AMPK, AMPK activation by ILQ seems to be independent of SIRT1–LKB1, as supported by our additional findings that ILQ unaffected LKB1 phosphorylation, and that AMPK activation was still observed in LKB1-deficient HeLa cells (data not shown). Furthermore, AMPKα phosphorylation by ILQ was transient at early times, which might be due to its LKB1 independency. CaMKK and transforming growth factor β-activated kinase-1 are other upstream kinases of AMPK [31,50]. Protein phosphatase 2C is a negative regulator of AMPK [51]. Therefore AMPK activation by ILQ may be associated with these targets. Nonetheless, cytoprotective effects and AMPK activation elicited by several phytochemicals (e.g., sauchinone

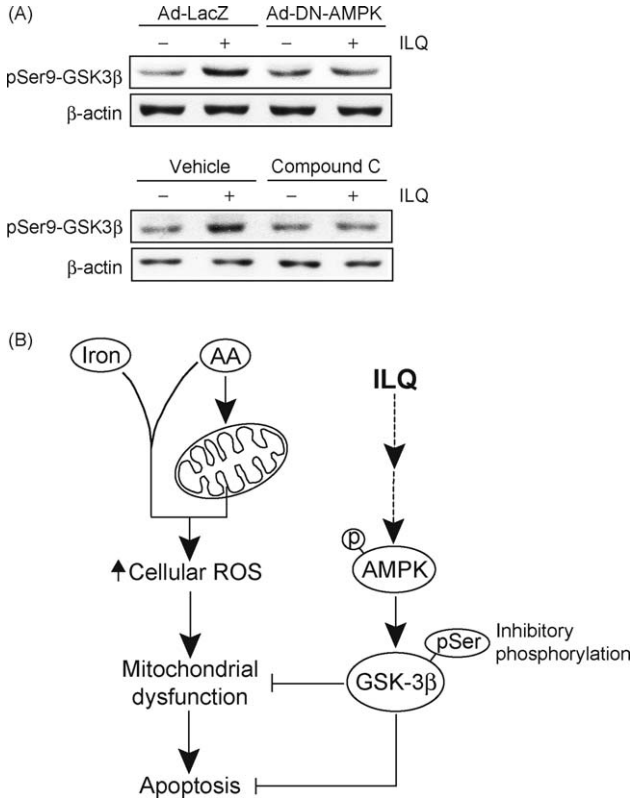

Fig. 7. AMPK-dependent GSK3β phosphorylation by ILQ. (A) Inhibition of ILQ-induced GSK3β phosphorylation by Ad-DN-AMPK transfection or compound C treatment. Cells were incubated with ILQ for 6 h following infection with Ad-DN-AMPK for 36 h or treatment with compound C for 30 min. Results were confirmed by repeated experiments. (B) A schematic diagram illustrating the proposed mechanism by which ILQ protects mitochondria and cells against toxicity induced by AA plus iron.

and resveratrol) may not be linked with these pathways [27,39]. The upstream target of ILQ for AMPK-GSK3β phosphorylation remains to be studied.

ILQ treatment activates Nrf2 possibly by altering Keap1 conformation [19,20]. In our study, we also found that ILQ induced Nrf2 and promoted its nuclear accumulation. However, the cytoprotective effect of ILQ was not reversed by siRNA knockdown of Nrf2 (data not shown). As the same token, enforced expression of Nrf2 was ineffective in protecting cells against oxidative stress caused by AA + iron (data not shown). Although the Nrf2–ARE pathway is considered as an important antioxidative basis, it may not be sufficient to protect mitochondria from severe oxidative stress elicited by iron catalysis. Taken together, our results demonstrate that ILQ protects cells from AA + iron-induced ROS production and mitochondrial dysfunction; a cytoprotective effect mediated via AMPK-dependent GSK3β inactivation. ILQ may be useful to protect mitochondria from an iron-catalyzed burst of oxidative stress, and thereby this agent may be utilized as a beneficial antioxidative candidate.

Conflict of interests

The authors declare that they have no conflict of interests.

Acknowledgment

This work was supported by the National Research Foundation of Korea grant funded by the Korea government (MEST) (No. 2009-0063233), Korea.

References

[1] Browning JD, Horton JD. Molecular mediators of hepatic steatosis and liver injury. J Clin Invest 2004;114:147–52.
[2] Balboa MA, Balsinde J. Oxidative stress and arachidonic acid mobilization. Biochim Biophys Acta 2006;1761:385–91.
[3] Jayadev S, Linardic CM, Hannun YA. Identification of arachidonic acid as a mediator of sphingomyelin hydrolysis in response to tumor necrosis factor alpha. J Biol Chem 1994;269:5757–63.
[4] Scorrano L, Oakes SA, Opferman JT, Cheng EH, Sorcinelli MD, Pozzan T, et al. BAX and BAK regulation of endoplasmic reticulum Ca^{2+}: a control point for apoptosis. Science 2003;300:135–9.
[5] Cocco T, Di Paola M, Papa S, Lorusso M. Arachidonic acid interaction with the mitochondrial electron transport chain promotes reactive oxygen species generation. Free Radic Biol Med 1999;27:51–9.
[6] Scorrano L, Penzo D, Petronilli V, Pagano F, Bernardi P. Arachidonic acid causes cell death through the mitochondrial permeability transition. Implications for tumor necrosis factor-alpha aopototic signaling. J Biol Chem 2001;276:12035–40.
[7] Shin SM, Kim SG. Inhibition of arachidonic acid and iron-induced mitochondrial dysfunction and apoptosis by oltipraz and novel 1,2-dithiole-3-thione congeners. Mol Pharmacol 2009;75:242–53.
[8] Haraguchi H, Ishikawa H, Mizutani K, Tamura Y, Kinoshita T. Antioxidative and superoxide scavenging activities of retrochalcones in *Glycyrrhiza inflata*. Bioorg Med Chem 1998;6:339–47.
[9] Chin YW, Jung HA, Liu Y, Su BN, Castoro JA, Keller WJ, et al. Anti-oxidant constituents of the roots and stolons of licorice (*Glycyrrhiza glabra*). J Agric Food Chem 2007;55:4691–7.
[10] Lee CK, Son SH, Park KK, Park JH, Lim SS, Chung WY. Isoliquiritigenin inhibits tumor growth and protects the kidney and liver against chemotherapy-induced toxicity in a mouse xenograft model of colon carcinoma. J Pharmacol Sci 2008;106:444–51.
[11] Kumar S, Sharma A, Madan B, Singhal V, Ghosh B. Isoliquiritigenin inhibits IkappaB kinase activity and ROS generation to block TNF-alpha induced expression of cell adhesion molecules on human endothelial cells. Biochem Pharmacol 2007;73:1602–12.
[12] Kim JY, Park SJ, Yun KJ, Cho YW, Park HJ, Lee KT. Isoliquiritigenin isolated from the roots of *Glycyrrhiza uralensis* inhibits LPS-induced iNOS and COX-2 expression via the attenuation of NF-κB in Raw264.7 macrophages. Eur J Pharmacol 2008;584:175–84.
[13] Takahashi T, Takasuka N, Iigo M, Baba M, Nishino H, Tsuda H, et al. Isoliquiritigenin, a flavonoid from licorice, reduces prostaglandin E2 and nitric oxide, causes apoptosis, and suppresses aberrant crypt foci development. Cancer Sci 2004;95:448–53.
[14] Lee YM, Lim do Y, Choi HJ, Jung JI, Chung WY, Park JH. Induction of cell cycle arrest in prostate cancer cells by the dietary compound isoliquiritigenin. J Med Food 2009;12:8–14.
[15] Tawata M, Aida K, Noguchi T, Ozaki Y, Kume S, Sasaki H, et al. Anti-platelet action of isoliquiritigenin, an aldose reductase inhibitor in licorice. Eur J Pharmacol 1992;212:87–92.
[16] Kim DC, Choi SY, Kim SH, Yun BS, Yoo ID, Reddy NR, et al. Isoliquiritigenin selectively inhibits H_2 histamine receptor signaling. Mol Pharmacol 2006;70:493–500.
[17] Lan F, Cacicedo JM, Ruderman N, Ido Y. SIRT1 modulation of the acetylation status, cytosolic localization, and activity of LKB1. Possible role in AMP-activated protein kinase activation. J Biol Chem 2008;283:27628–35.
[18] Howitz KT, Bitterman KJ, Cohen HY, Lamming DW, Lavu S, Wood JG, et al. Small molecule activators of sirtuins extend *Saccharomyces cerevisiae* lifespan. Nature 2003;425:191–6.
[19] Luo Y, Eggler AL, Liu D, Liu G, Mesecar AD, van Breemen RB. Sites of alkylation of human Keap1 by natural chemoprevention agents. J Am Soc Mass Spectrom 2007;18:2226–32.
[20] Kobayashi M, Li L, Iwamoto N, Nakajima-Takagi Y, Kaneko H, Nakayama Y, et al. The antioxidant defense system Keap1-Nrf2 comprises a multiple sensing mechanism for responding to a wide range of chemical compounds. Mol Cell Biol 2009;29:493–502.
[21] Kockeritz L, Doble B, Patel S, Woodgett JR. Glycogen synthase kinase-3—an overview of an over-achieving protein kinase. Curr Drug Targets 2006;7:1377–88.
[22] Grimes CA, Jope RS. The multifaceted roles of glycogen synthase kinase 3 beta in cellular signaling. Prog Neurobiol 2001;65:391–426.
[23] Tong H, Imahashi K, Steenbergen C, Murphy E. Phosphorylation of glycogen synthase kinase-3β during preconditioning through a phosphatidylinositol-3-kinase-dependent pathway is cardioprotective. Circ Res 2002;90:377–9.
[24] Park SS, Zhao H, Mueller RA, Xu Z. Bradykinin prevents reperfusion injury by targeting mitochondrial permeability transition pore through glycogen synthase kinase-3β. J Mol Cell Cardiol 2006;40:708–16.
[25] Das S, Wong R, Rajapakse N, Murphy E, Steenbergen C. Glycogen synthase kinase 3 inhibition slows mitochondrial adenine nucleotide transport and regulates voltage-dependent anion channel phosphorylation. Circ Res 2008;103:983–91.
[26] Nishihara M, Miura T, Miki T, Tanno M, Yano T, Naitoh K, et al. Modulation of the mitochondrial permeability transition pore complex in GSK-3β-mediated myocardial protection. J Mol Cell Cardiol 2007;43:564–70.
[27] Shin SM, Cho IJ, Kim SG. Resveratrol protects mitochondria against oxidative stress through AMPK-mediated GSK3β inhibition downstream of poly(ADP-ribose)polymerase-LKB1 pathway. Mol Pharmacol 2009;76:884–95.

[28] Hayashi T, Hirshman MF, Fujii N, Habinowski SA, Witters LA, Goodyear LJ. Metabolic stress and altered glucose transport: activation of AMP-activated protein kinase as a unifying coupling mechanism. Diabetes 2000;49:527–31.
[29] Terai K, Hiramoto Y, Masaki M, Sugiyama S, Kuroda T, Hori M, et al. AMP-activated protein kinase protects cardiomyocytes against hypoxic injury through attenuation of endoplasmic reticulum stress. Mol Cell Biol 2005;25:9554–75.
[30] Woods A, Johnstone SR, Dickerson K, Leiper FC, Fryer LG, Neumann D, et al. LKB1 is the upstream kinase in the AMP-activated protein kinase cascade. Curr Biol 2003;13:2004–8.
[31] Hawley SA, Pan DA, Mustard KJ, Ross L, Bain J, Edelman AM, et al. Calmodulin-dependent protein kinase kinase-β is an alternative upstream kinase for AMP-activated protein kinase. Cell Metab 2005;2:9–19.
[32] Ido Y, Carling D, Ruderman N. Hyperglycemia-induced apoptosis in human umbilical vein endothelial cells: inhibition by the AMP-activated protein kinase activation. Diabetes 2002;51:159–67.
[33] Detaille D, Guigas B, Chauvin C, Batandier C, Fontaine E, Wiernsperger N, et al. Metformin prevents high-glucose-induced endothelial cell death through a mitochondrial permeability transition-dependent process. Diabetes 2005;54:2179–87.
[34] Adachi M, Brenner DA. High molecular weight adiponectin inhibits proliferation of hepatic stellate cells via activation of adenosine monophosphate-activated protein kinase. Hepatology 2008;47:677–85.
[35] Blois MS. Antioxidant determinations by the use of a stable free radical. Nature 1958;181:1199–200.
[36] Molyneux P. The use of the stable free radical diphenylpicrylhydrazyl (DPPH) for estimating antioxidant activity. J Sci Technol 2004;26:211–9.
[37] Lemasters JJ, Nieminen AL. Mitochondrial oxygen radical formation during reductive and oxidative stress to intact hepatocytes. Biosci Rep 1997;17:281–91.
[38] Kode A, Rajendrasozhan S, Caito S, Yang SR, Megson IL, Rahman I. Resveratrol induces glutathione synthesis by activation of Nrf2 and protects against cigarette smoke-mediated oxidative stress in human lung epithelial cells. Am J Physiol Lung Cell Mol Physiol 2008;294:L478–88.
[39] Kim YW, Lee SM, Shin SM, Hwang SJ, Brooks JS, Kang HE, et al. Efficacy of sauchinone as a novel AMPK-activating lignan for preventing iron-induced oxidative stress and liver injury. Free Radic Biol Med 2009;47:1082–92.
[40] McLaren CE, Gordeuk VR, Looker AC, Hasselblad V, Edwards CQ, Griffen LM, et al. Prevalence of heterozygotes for hemochromatosis in the white population of the United States. Blood 1995;86:2021–7.
[41] Galaris D, Pantopoulos K. Oxidative stress and iron homeostasis: mechanistic and health aspects. Crit Rev Clin Lab Sci 2008;45:1–23.
[42] Neufeld EJ. Oral chelators deferasirox and deferiprone for transfusional iron overload in thalassemia major: new data, new questions. Blood 2006;107:3436–41.
[43] Zamzami N, Kroemer G. The mitochondrion in apoptosis: how Pandora's box opens. Nat Rev Mol Cell Biol 2001;2:67–71.
[44] Muralikrishna Adibhatla R, Hatcher JF. Phospholipase A2, reactive oxygen species, and lipid peroxidation in cerebral ischemia. Free Radic Biol Med 2006;40:376–87.
[45] Juhaszova M, Zorov DB, Kim SH, Pepe S, Fu Q, Fishbein KW, et al. Glycogen synthase kinase-3beta mediates convergence of protection signaling to inhibit the mitochondrial permeability transition pore. J Clin Invest 2004;113:1535–49.
[46] Horike N, Sakoda H, Kushiyama A, Ono H, Fujishiro M, Kamata H, et al. AMP-activated protein kinase activation increases phosphorylation of glycogen synthase kinase 3β and thereby reduces cAMP-responsive element transcriptional activity and phosphoenolpyruvate carboxykinase C gene expression in the liver. J Biol Chem 2008;283:33902–10.
[47] Shaw RJ, Kosmatka M, Bardeesy N, Hurley RL, Witters LA, DePinho RA, et al. The tumor suppressor LKB1 kinase directly activates AMP-activated kinase and regulates apoptosis in response to energy stress. Proc Natl Acad Sci U S A 2004;101:3329–35.
[48] Kukidome D, Nishikawa T, Sonoda K, Imoto K, Fujisawa K, Yano M, et al. Activation of AMP-activated protein kinase reduces hyperglycemia-induced mitochondrial reactive oxygen species production and promotes mitochondrial biogenesis in human umbilical vein endothelial cells. Diabetes 2006;55:120–7.
[49] Hou X, Xu S, Maitland-Toolan KA, Sato K, Jiang B, Ido Y, et al. SIRT1 regulates hepatocyte lipid metabolism through activating AMP-activated protein kinase. J Biol Chem 2008;283:20015–26.
[50] Momcilovic M, Hong SP, Carlson M. Mammalian TAK1 activates Snf1 protein kinase in yeast and phosphorylates AMP-activated protein kinase in vitro. J Biol Chem 2006;281:25336–43.
[51] Davies SP, Helps NR, Cohen PT, Hardie DG. 5′-AMP inhibits dephosphorylation, as well as promoting phosphorylation, of the AMP-activated protein kinase. Studies using bacterially expressed human protein phosphatase-2C alpha and native bovine protein phosphatase-2AC. FEBS Lett 1995;377:421–5.